

Supplementary Information

Directional bounce of droplets on oblique two-tiers conical structures

Dan Li, Shile Feng, Yan Xing, Siyan Deng, Hu Zhou, Yongmei Zheng*

Key Laboratory of Bio-Inspired Smart Interfacial Science and Technology of Ministry of Education, School of Chemistry and Environment, Beihang University, Beijing, 100191, P. R. China.

*E-mail: zhengym@buaa.edu.cn.

Contents:

Experimental Section

Supplementary Figure Legends: (Figure S1-S8)

Supplementary Analysis

Experimental Section:

Preparation of oblique two-tiers conical structures (OTCS): A commercial sewing needle was attached to a jet dispensing system to prick regular holes array on a piece of PE sheet. The mixture (weight ratio of 2:1) of PDMS pre-polymer (contained 0.1 equivalent curing agents, SYLGARD 184) and Co nanoparticles was used to replicate the holes array on PE sheet. The magnetically PDMS vertical conical structures obtained after curing. The magnetically vertical conical structures tilted out from the original z -axis orientation into the x-y plane and become oblique conical structures (OCS) because of the influence of the magnetic field of the permanent magnet. During the fabrication process of OCS with oblique angle (OA) of 75° (see Figure S2a), the magnet was placed vertically and the magnetic field lines are vertical (the north magnetic pole was upward and the south magnetic pole was downward). The vertical conical structures were placed on the north magnetic pole and then one side of the sample was uplifted to keep an angle of 15° between the sample and the surface of magnet. During the fabrication process of OCS with OA of 60° (see Figure S2b), the magnet was placed horizontally and the magnetic field lines are horizontal. The vertical conical structures were horizontal placed next to the south magnetic pole. The distance between the sample and the south magnetic pole was expanded slightly to fabricate OCS with OA of 45°. Then tri (propyleneglycol) diacrylate (TPGDA) diluted by xylene was used to replicate the OCS and generated a template with neat cavities after curing. The PDMS was poured to cover the template, after curing it was peeled off prudently along the orientation of the OCS. The OCS were obtained, then that were washed with acetone, ethanol and deionized water in ultrasonic cleaner for 5 min, and dried in a drying oven. The crystal seed solution was prepared as follows: 3 g of $\text{Zn}(\text{Ac})_2 \cdot 2\text{H}_2\text{O}$, 20 mL of ethylene glycol monomethyl ether and 0.8 g of monoethanolamine were mixed and stirred with a magnetic stirrer for 30 min. The growth liquid was prepared as follows: 0.74 g of $\text{Zn}(\text{NO}_3)_2 \cdot 6\text{H}_2\text{O}$ and 0.35 g of hexamethylene tetramine were mixed with 100 mL of deionized water and stirred until becoming a transparent solution. The surface of OCS was covered with a layer of crystal seed solution by dip-coating method two times, then OCS were put into a muffle furnace horizontally at 350°C for 2 min. After that, OCS were put into the reaction kettle perpendicularly and the growth liquid was added slowly. The reaction kettle was put in an oven at 90°C for 10 h. After, OTCS were fabricated and removed from the reactor and washed with deionized water, and subsequently dried in an oven. OTCS were cleaned with plasma cleaning (PDC-32G, HARRICK PLSMA) at middle power for 5 min to enhance their chemical activities. Finally OTCS were put into a vacuum drier which there were two drops of heptadecafluorodecyltripropoxysilane (FAS-17). The vacuum drier was placed under reduced pressure to -0.1 MPa and kept in an oven at 90°C for 6 h without light. The

resulting surfaces have a low surface energy chemical component. Finally, the OTCS with low surface energy were obtained.

Instruments and Characterization: The surface morphologies of samples were observed by a microscope (G-120A, China) and environmental scanning electron microscope (ESEM, Quanta FEG 250, FEI) at 10 kV. The static contact angles, rolling-off angles of droplets were measured by the optical contact angle meter (OCA40Micro, Data physics Instruments GmbH, Germany). The dynamic processes of droplets bouncing were recorded by high-speed CCD camera (Phantom v9.1, Vision Research, USA). The continuous self-propelled bouncing action of the droplet was observed by the camera (Canon 750D, Japan). The energy dispersive X-ray spectroscopy (EDX) was tested by Scanning Electron Microscopy (INCA Energy 250, OXFORD INSTRUMENTS). The X-ray diffraction (XRD) (JCPDS Card No. 36-1451) was used to confirm the formation of ZnO nano-hairs.

Supplementary Figure Legends:

Figure S1

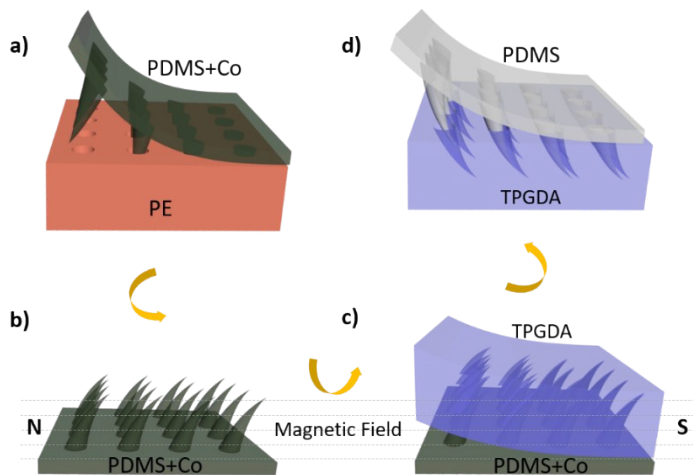


Figure S1. (a) The structures replicating by a mixture of PDMS+Co. (b) The vertical cone arrays change into oblique cone arrays because the influence of the magnetic field. (c) TPGDA replicating the oblique PDMS cones arrays. (d) The PDMS pre-polymer covering the template with neat cavities. After curing, PDMS is peeled off prudently along the orientation of the oblique conical structures.

Figure S2

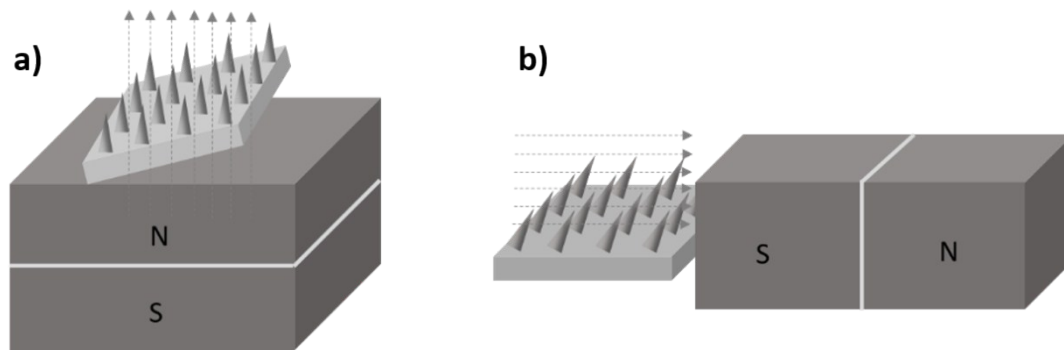


Figure S2. The relationship between OA and magnetic field during the fabrication process of OCS.

Figure S3

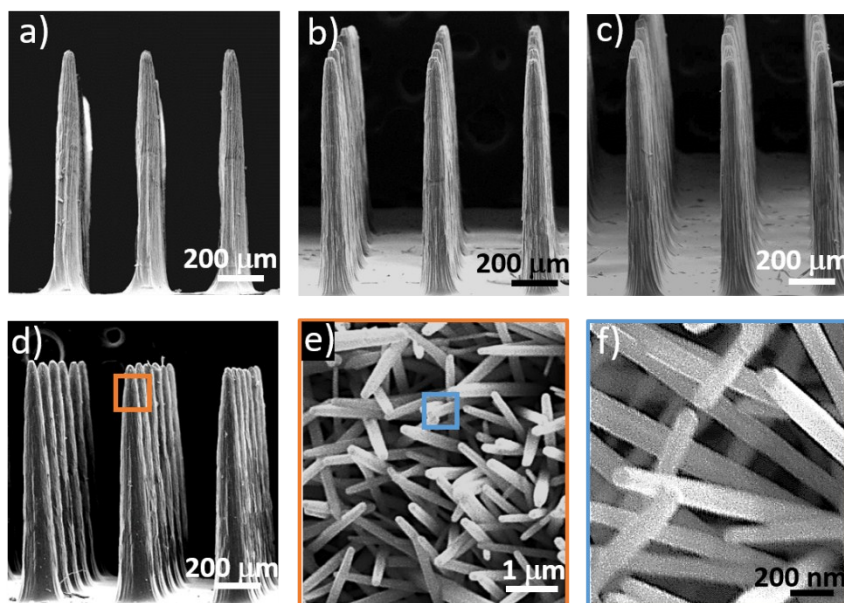


Figure S3. The SEM images of the VTCS covered with ZnO nano-hairs. (a - d) SEM images in the side view of the VTCS with different periodicities (350 μm, 400 μm, 450 μm and 500 μm). The base diameter of the cone is 200 μm, and the height of the cone structure is 1 mm. (e – f) SEM images in high magnification, the surface was covered by ZnO nano-hairs. The diameters of ZnO are ~ 100 nm and the lengths are ~ 1 μm on average, respectively.

Figure S4

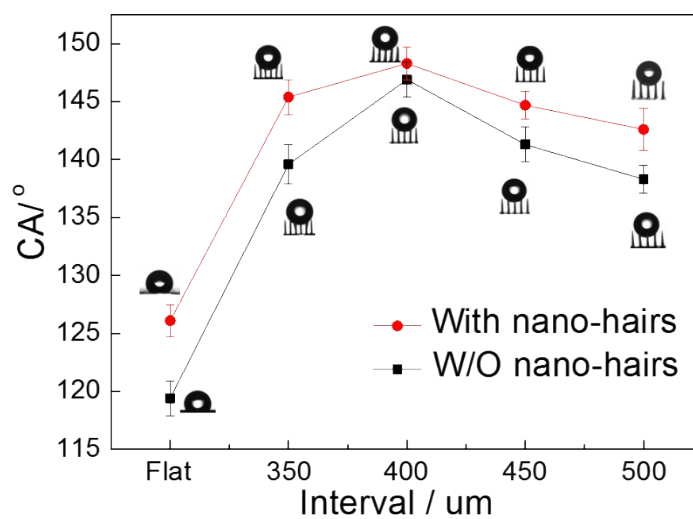


Figure S4 Static CAs of the droplet on the vertical conical structures with/ without nano-hairs at different periodicities (350 μm , 400 μm , 450 μm and 500 μm). The CAs of VTCS are higher than the vertical conical structures. When periodicity of 400 μm , the CA is largest.

Figure S5

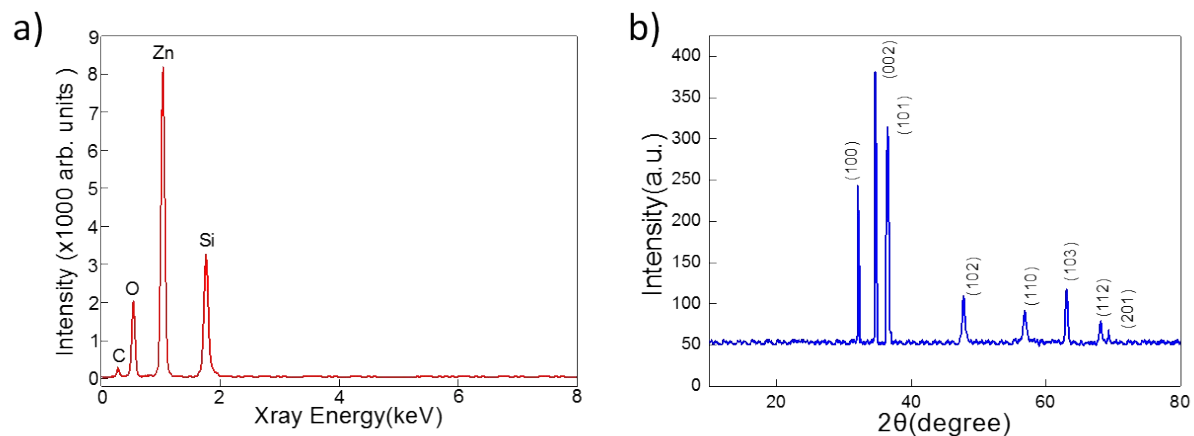


Figure S5 The energy dispersive X-ray spectroscopy (EDX) and the X-ray diffraction (XRD) patterns of OTCS surface. (a) The EDX results are consistent with the components of OTCS (PDMS: Si, O, C and ZnO: Zn, O). (b) The XRD pattern confirms the formation of ZnO nanorods. Obviously, no apparent diffraction peak can be identified at the spectrum, which indicates that OTCS surface is covered by ZnO nanohairs.

Figure S6

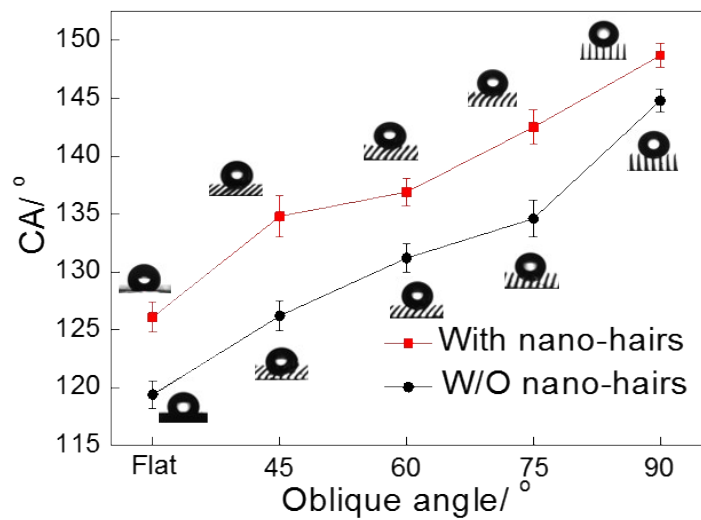


Figure S6. Static CAs on the OTCS. Static CAs of the droplets on the oblique conical structures with/ without nano-hairs at different oblique angles (OAs) (flat, 45°, 60°, 75°, 90°). The CAs of OTCS are higher than the oblique conical structures without nano-hairs accordingly. In addition, the CAs of OTCS are lower than the vertical and decrease with the minish of the OAs.

Figure S7

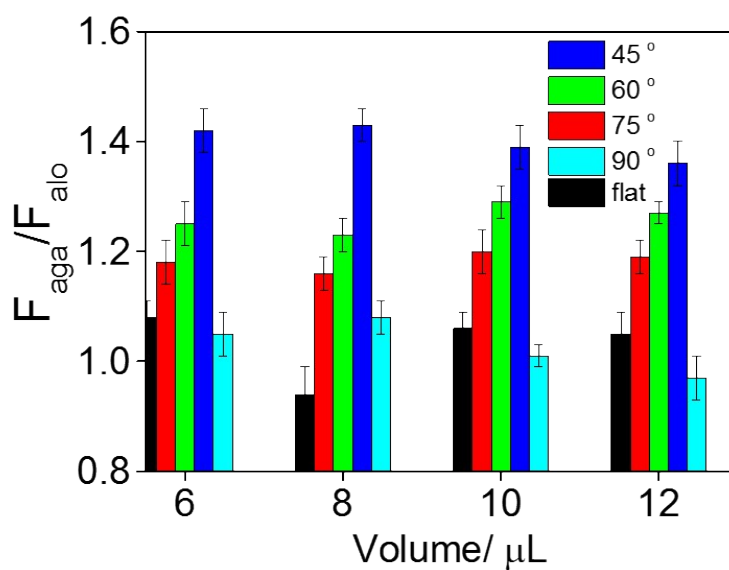


Figure S7. The ratio F_{aga}/F_{alo} as functions of droplet volume. For the flat PDMS and vertical array (i.e., OA_(90°)), the ratios of F_{aga} to F_{alo} are around 1, with the averages of 1.0275 and 1.0325. The ratios of F_{aga} to F_{alo} for OA_(75°) to OA_(45°) are range from 1.18 to 1.40, and the ratios increase with the decrease of OAs.

Figure S8

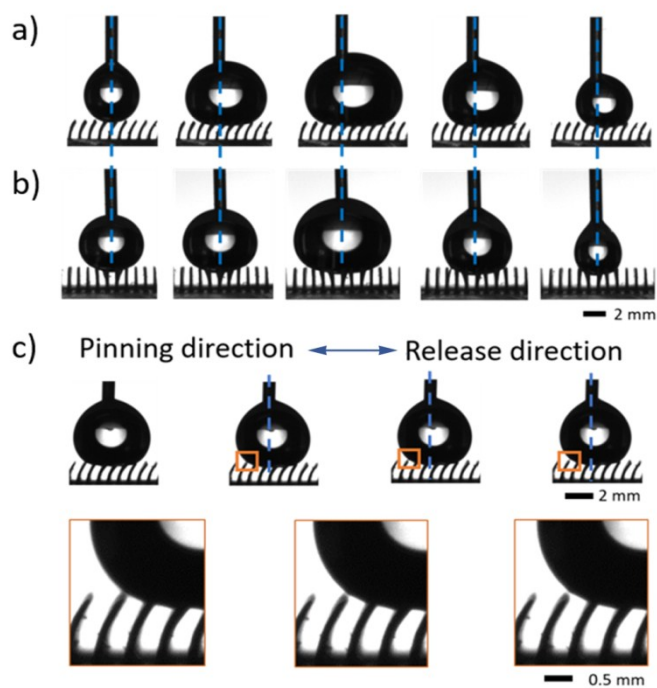


Figure S8. Observation on dynamic CAs on OTCS. (a) On the OTCS, the center of the drop moves toward the release direction in advancing process and it doesn't recover in receding process. (b) On VTCS, the shape of drop keeps symmetric in advancing and receding process. (c) Observation on dynamic receding process of a droplet, the contact line breaking away from release direction rather than pinning direction preferentially.

Supplementary Analysis

1 The wettability and anisotropic of the OTCS

Firstly, the wettability on OTCS with different OAs is investigated. The static CAs of droplets with 3 μL are observed by sessile drop method, as shown in Figure S6. The CA of flat PDMS is $119^\circ \pm 1.2^\circ$, which shows hydrophobicity. Compared to flat PDMS, cone-shaped PDMS has higher CA and its hydrophobicity increases markedly. For the conical PDMS, air can be trapped in the micro structures therefore the contact between the solid surface and liquid is discrete. The liquid–solid contact lines of water droplets are reduced and thus the hydrophobicity is improved¹. The micro cone-shaped structures transfer droplets from the Wenzel² state to Wenzel-Cassia³ compounded state. In addition, the CA of oblique conical structures are lower than the vertical and decreasing with the OAs. Since droplets on the oblique cones, the contact part between the solid and liquid is larger than droplets on the vertical cones, and solid-liquid-gas three phase contact lines (TCLs) are increase with the decrease of OAs. When the flat PDMS is covered with ZnO nano-hairs, the CAs increase to $126.1^\circ \pm 1.3^\circ$ and the sample is more hydrophobic. Concurrently, the CAs of VTCS and OTCS are higher than the original structures accordingly, which show super-hydrophobicity. This indicatives the importance of nanostructures in building super-hydrophobic surfaces. The surfaces of the structures are covered with ZnO nano-hairs to reduce TCLs around droplets, which maintains droplets in Cassie state. Micro/nano-scale two-tiers structures are really the key structural features which allowed surfaces to remain super-hydrophobicity¹.

$$F = \rho V g \sin \alpha \quad (1)$$

Where V is the volume of droplet, ρ is the density of water, g is the gravitational acceleration. The retention forces for 6-12 μL droplets against/ along the oblique direction (OD) are represented as F_{against} (F_{aga}) and F_{along} (F_{alo}) (Figure S7). For the flat PDMS and VTCS, the ratios of F_{aga} to F_{alo} are around 1, with the averages of 1.0275 and 1.0325. In contrast, the ratios of F_{aga} to F_{alo} for OTCS with different OAs (75° to 45°) are range from 1.18 to 1.40, and the ratios increase with the decrease of OAs. When the volume of a droplet increases or decreases, the contact part of solid and liquid changes relatively. For VTCS, the TCLs elongate or minish symmetrically during the increasing or decreasing process (Figure S8b). But for OTCS, the deformation of the TCLs happens. Figure S8a shows that the skewing of the center of the droplet happens during the droplet increasing. The droplet shifts toward to the oblique direction of the micro structures and the TCLs elongate asymmetrically. Subsequently the volume of the droplet decreases, thus the contact part of solid and liquid shrinks and the TCLs remain asymmetrical. During

the decreasing of the droplet, the shrinking is asymmetrical, (Figure S8c) the contact line breaks away from release direction rather than pinning direction preferentially.

2 The mechanism of ZnO nano-hairs growth

The mechanism of ZnO nano-hairs growth can be divided into two steps. The first step is precipitation reaction, hexamethylene tetramine hydrolysis into $\text{NH}_3 \cdot \text{H}_2\text{O}$ and HCHO. Under alkaline condition, Zn^{2+} and OH^- combine into $\text{Zn}(\text{OH})_2$ and $[\text{Zn}(\text{OH})_4]^{2-}$. The second step is dehydration reaction. $\text{Zn}(\text{OH})_2$ and $[\text{Zn}(\text{OH})_4]^{2-}$ dehydrate into ZnO under heated condition. The XRD pattern⁴ confirms the formation the formation ZnO nano-hairs as hexagonal wurtzite structure.

References

- 1 B. Su, Y. Tian and L. Jiang, *J. Am. Chem. Soc.*, 2016, 138, 1727-1748.
- 2 R. N. Wenzel, *Ind. Eng. Chem.*, 1936, 28, 988-994.
- 3 A. B. D. Cassie and S. BaxtER, *Trans. Faraday Soc.*, 1944, 40, 546-551.
- 4 M. Q. Zhang, L. Wang, S. L. Feng and Y. M. Zheng, *Chem. Mater.*, 2017, 29 (7), 2899-2905.